

# Heat Transfer and Fluid Flow in Double Pipe Heat Exchanger, Part II: Numerical Investigation

Shreyas Kotian<sup>1</sup>, Nachiket Methekar<sup>2</sup>, Nishant Jain<sup>3</sup> and Prithish Naik<sup>4</sup>

<sup>1,2,3&4</sup>Department of Mechanical Engineering, K.J. Somaiya College of Engineering, Mumbai, India.  
 E-mail: shreyas.kotian@somaiya.edu

(Received 30 September 2020; Revised 23 October 2020; Accepted 15 November 2020; Available online 23 November 2020)

**Abstract** - Analysis of thermo hydraulic characteristics in a simple configuration of the double-pipe heat exchangers adds a great value to the design of heat exchangers. This paper presents a comparison of the experimental observations and numerical predictions for the thermal characteristics of the double pipe heat exchanger. A CAD design was developed and the Realizable k- $\epsilon$  mathematical model coupled with enhanced wall treatment gave the closest results. Experiments were performed for  $60 \leq Re \leq 240$  for two different inlet temperatures of the hot fluid,

50°C, and 70°C keeping the inlet temperature of the cold fluid constant at 31°C. Temperature gradients extracted from ANSYS Fluent were compared with the experimental data. Further, pressure and temperature contours for the hot and cold streams were generated to analyze the performance parameters.

**Keywords:** Double pipe heat exchanger, CAD design, ANSYS FLUENT, thermo hydraulic characteristics

## NOMENCLATURE

Abbreviations		t	Time [s]
CFD	Computational Fluid Dynamics	$b_x, b_y, b_z$	Body forces in x, y, z directions respectively
FVM	Finite Volume Method	<i>Superscripts and subscripts</i>	
FEM	Finite Element Analysis	c	Cold stream
FDM	Finite Difference Analysis	h	Hot stream
BEM	Boundary Element Analysis	i	Inlet
CAD	Computer Aided Design	o	Outlet
PDE	Partial Differential Equation	<i>Greeks and symbols</i>	
u, v, w	Components of velocity in x, y, z direction respectively [m/s]	$\rho$	Density (kg/m <sup>3</sup> )
Q	Volume flow rate [lpm]	$\mu$	Dynamic viscosity [kg/m s]
T	Temperature [°C]	$\emptyset$	Dissipation Function
p	Pressure [Pa]		

## I. INTRODUCTION

Heat exchangers are the devices that provide the transfer of thermal energy between two or more fluids at different temperatures. They find applications in power production, chemical and food industries, environmental engineering, and waste heat recovery. Perhaps, the simplest of these heat exchangers is the double pipe heat exchanger. Advantages include ease of cleaning and maintenance and usage under severe fouling conditions. Fluids at high pressure can also be used. Limitations include difficulty in the cleaning of tubes due to fouling and a shell and tube heat exchanger of the same design is a better way for heat transfer. This present study will investigate the comparison of numerical results with experimental data of a double pipe heat exchanger. Many researchers have investigated the

Thermo hydraulic performance of the double pipe heat exchanger which is presented in this section.

Shirvan *et al* [5]. studied the enhancement of heat transfer and effectiveness in a double pipe heat exchanger filled with porous media. Simulations were performed for  $3000 \leq Re \leq 5000$  and  $10^{-5} \leq Da \leq 10^{-3}$ . It was found that the mean Nu increases with increasing Re and the reduction in Da and porous substrate thickness. Effectiveness would be maximized when  $Re = 5000$ ,  $Da = 10^{-3}$  and  $\delta = 1$ . At  $Re = 5000$ ,  $Da = 10^{-3}$  and  $\delta = 1$  Nu and effectiveness were maximized simultaneously. Maakoul *et al* [6]. investigated the thermohydraulic characteristics of the double pipe heat exchanger with split longitudinal fins on the annulus side. It was found that the SLF had the advantage to repeat an entrance region-like effect along with the flow of the length. The results showed that the heat transfer rates in annulus equipped with SLF are higher than those with conventional

LF by 31%–48% for the same pumping power and unit weight. Cavazzuti *et al* [7]. Proposed an efficient method to optimize finned double pipe heat exchanger in industrial recuperative burners. It was intended to maximize the heat transfer, compactness, and pressure drop constraints. The optimum configurations enhanced the thermal performance by 10.8%. Timothy *et al* [8]. installed vortex generators with the triangular cross-section along the centreline of the helical channel of the double pipe heat exchanger and it was found that the heat transfer was augmented by 16.6%. Thus, it was concluded that helical fins with the addition of vortex generators would greatly improve the effectiveness of the heat exchanger. Maakoul *et al* [9]. studied the thermo hydraulic performance of a proposed design of an air-to-water double pipe heat exchanger with helical fins on the annulus gas side, numerically.

It was found that the overall compactness and performance of the heat exchanger improves through the use of fins and a fin spacing of 0.1m provides the optimal thermo hydraulic performance. Maakoul *et al* [10]. also studied the design and thermo-hydraulic performance of a double pipe heat exchanger with helical baffles in the annulus side numerically. Helically baffled fins provided enhanced heat transfer than the simple double pipe heat exchangers. It was also found out that thermal performance and high-pressure drop is an increasing function of Re and baffle spacing.

Sheikholeslami *et al* [11]. Investigated the effect of typical and perforated conical ring tabulators on hydrothermal behaviour of air to water double pipe heat exchanger. Two arrays (Direct conical ring (DCR) array and Reverse conical ring (RCR) array) were considered. Results indicated that friction factor reduces with augment of open area ratio, pitch ratio, and Re while Nu follows the opposite trend. It was also found that thermal performance rose with increasing the conical angle for direct conical ring array. Tu *et al* [12]. carried out numerical investigations for turbulent flow in a circular pipe with pipe inserts.

The heat transfer rate decreases with the increase in spacer length. Compared with three pipes inserts, four pipes inserts have a better heat transfer performance, especially at high Reynolds number. The maximal PEC (Performance evaluation criterion) values resulted from four pipes inserts were approximately 1.4-3.0. Bezaatpour and Goharkhah [13]. have proposed an innovative method to improve convective heat transfer and also reduce pressure drop penalty. This is done by applying an external magnetic field to generate swirling flow in the magnetic working fluid. Using this application heat transfer was augmented by 320% and pressure drop was minimized due to the lack of any additional obstacle in the flow passage. Bashtani and Esfahani [14]. numerically investigated a double pipe heat exchanger with a simple and corrugated tube assuming three different wave amplitudes. The results show that, in a similar Re, corrugating increases Nusselt number so that at the maximum state the average Nusselt number of the

corrugated heat exchanger is about 1.75 times as compared to the simple heat exchanger. Compared to the simple heat exchanger, the ratio of effectiveness and second law efficiency of thermodynamics of the corrugated heat exchanger is 1.73 and 1.17, respectively. Zhang *et al* [15]. experimentally investigated thermal characteristics of a double-pipe heat exchanger fitted with perforated self-rotating twisted tapes with six perforation ratios of 0%, 1.16%, 3.63%, 6.46%, 10.1%, and 14.49%. Perforated self-rotating twisted tapes were experimentally shown to perform greater thermal performance than perforated stationary twisted tapes. When the self-rotating twisted tapes varied from stationary to rotating condition, it is observed that thermal performance factor increased from 0.862 to 0.924, 0.987 to 1.025, 1.04 to 1.078, 1.084 to 1.101, and 1.042 to 1.055, for perforation ratios of 0%, 1.16%, 3.63%, 6.46%, and 10.1%, respectively.

Sharifi *et al* [16]. studied the influence of coiled wire inserts on Nu, friction coefficient, and overall efficiency. It was found out that with the proper use of coil inserts the Nu could improve over 1.77 times. Following this numerical simulation friction coefficient and Nu correlations were proposed. Wijayanta *et al* [17]. tried to enhance the heat transfer using double-sided delta wing tape inserts. Investigations were done for  $5300 \leq Re \leq 14,500$ . The T-W tape insert (wing-width ratio: 0.63) resulted in the highest average Nusselt number, where the average Nusselt number is higher by 177% relative to that for the plain tube.

The T-W tape insert (wing-width ratio: 0.63) also results in the highest thermal performance factor (1.15) and Nu, the thermal performance factor increases as the wing-width ratio of the T-Ws increases. Bazgir *et al* [18]. proposed that the thermal efficiency and performance of a counter-flow vortex tube can be improved by cooling the main or hot-tube of the vortex tube. It was concluded that cooling the hot-tube helps in increasing the cold air temperature difference,  $\Delta T_c$ , and improving isentropic efficiency of the system. The vortex tube with cooling water possesses higher cold air temperature differences and efficiencies than the one without cooling water by 6.3–10.3% and 5.8–10.6%, respectively.

Gorman *et al* [19]. investigated the thermal and fluid flow design of a double-pipe heat exchanger in which the wall of the inner pipe is helically corrugated. Two thermal-hydraulic models were employed.

Comparisons with simple smooth-walled double-pipe exchangers showed roughly a factor of three increases in heat transfer for the helically corrugated double-pipe heat exchangers. The counter-flow operation yielded higher rates of heat transfer, but to an extent that depends on whether the fluid properties are temperature-dependent or constant. Reynolds numbers for the investigated cases ranged from 420 to 2000.

## II. GEOMETRY OF THE HEAT EXCHANGER

The below table outlines the geometrical dimensions of the double pipe heat exchanger used in the present investigation.

TABLE 1 GEOMETRICAL PARAMETERS OF THE DOUBLE PIPE HEAT EXCHANGER UNDER INVESTIGATION

Parameters	Magnitude (Unit)/ Description
Inner Diameter of Inner Tube	26 mm
Outer Diameter of Inner Tube	34 mm
Thickness of Inner Tube	4 mm
Inner Diameter of Outer Tube	68 mm
Outer Diameter of Outer Tube	76 mm
Thickness of Outer Tube	4 mm
Length of inner and outer tube	1200 mm
Material of Inner and Outer Tube	Galvanized Iron

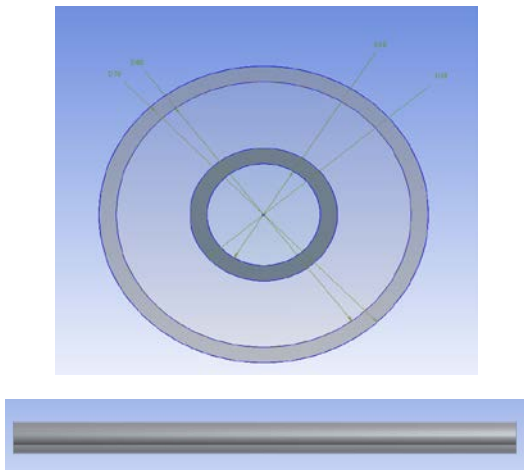


Fig. 1. Double pipe heat exchanger used for the present study

## III. METHODOLOGY

A numerical model has been developed to analyze the performance of the double pipe heat exchanger and the results have been compared with the experimental data. More details of the same have been mentioned in the following section.

### A. CFD Methodology

#### 1. Mathematical Model

In the present study, a double pipe heat exchanger was modelled using SOLIDWORKS, and meshing was done using ANSYS 2020 R1. The geometric model of STHX with the geometry mentioned in Table 1 is shown in Fig. 2.

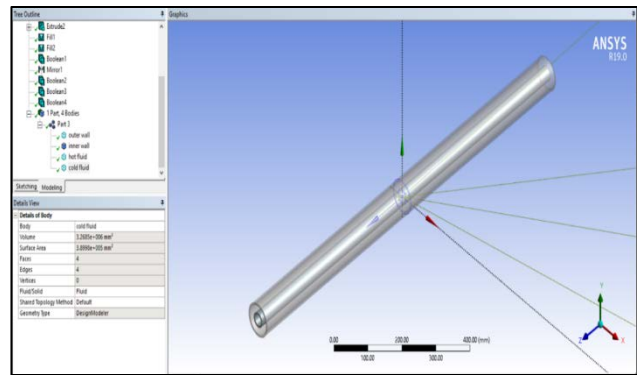


Fig. 2 3D model of the double pipe heat exchanger.

### 2. Mesh Topology

Meshing is nothing but discretization of a continuous body into a finite number of elements. The meshing was done using the ANSYS Meshing tool. The final mesh is obtained as a result of face, edge, and inflation types of meshing. Face meshing refines the elements on the face to obtain equal sized discrete parts that are easily realizable.

Edge meshing on both the inner and outer pipes is used to equalize the mesh sizes at the inlet and outlet lips of the tubes. Inflation boundaries are created on the outer side of the inner tube. A group of 4 discrete layers can be seen above. This is done to refine the results at the interface where heat exchange between two fluids takes place. This combination proves to be both very effective for the required accuracy and easy to process.

Fig. 3 shows a sectional view along a cut plane to show the final mesh obtained.

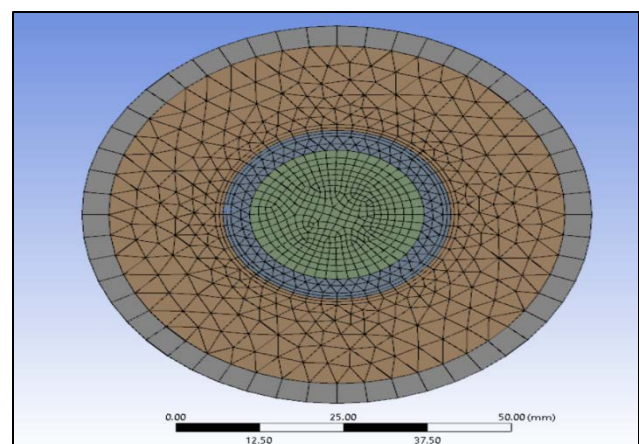


Fig. 3 Mesh obtained after applying map, face, and edge meshing

### 3. Governing Equations

The k-epsilon ( $k-\epsilon$ ) model for turbulence is the most common to simulate the mean flow characteristics. This is a 2-equation model that gives a general description of

turbulence using two transport equations (PDEs), which accounts for the effects like convection and diffusion of turbulent energy. The 2 transported variables are turbulent kinetic energy  $k$ , which determines the energy in turbulence, and turbulent dissipation  $\epsilon$ , which determines the rate of dissipation of the turbulent kinetic energy.

The  $k$ - $\epsilon$  model is shown to be applicable for free-shear flows, such as the ones with relatively small pressure gradients, but might not be the best model for problems involving large adverse pressure gradients. This model was based on numerical simulation of continuity, momentum, and energy equations.

Continuity equation:

$$\frac{\partial u_i}{\partial x_i} = 0$$

Momentum equation:

$$\frac{\partial u_i u_j}{\partial x_i} = -\frac{\partial \rho}{\rho \partial x_i} + \frac{\partial}{\partial x_j} \left( (v + v_t) \left( \frac{\partial u_j}{\partial x_i} + \frac{\partial u_i}{\partial x_j} \right) \right)$$

Energy equation:

$$\frac{\partial u_i T}{\partial x_i} = \rho \frac{\partial}{\partial x_i} \left( \left( \frac{v}{Pr} + \frac{v_t}{Pr_t} \right) \frac{\partial T}{\partial x_i} \right)$$

Turbulent kinetic energy  $k$  equation

$$\frac{\partial u_i k}{\partial x_i} = \frac{\partial}{\partial x_i} \left( \left( v + \frac{v_t}{\sigma_k} \right) \frac{\partial k}{\partial x_i} \right) + \Gamma - \epsilon$$

Rate of energy dissipation  $\epsilon$  equation

$$\frac{\partial \rho u_j}{\partial x_j} = \frac{\partial}{\partial x_i} \left( \left( v + \frac{v_t}{\sigma_k} \right) \frac{\partial \epsilon}{\partial x_i} \right) + C_1 \Gamma \epsilon - C_2 \frac{\epsilon^2}{k + \sqrt{v \epsilon}}$$

Where  $\Gamma$  denotes the production rate of  $k$  and is given by

$$\Gamma = -\bar{u}_i \bar{u}_j \frac{\partial u_i}{\partial x_i} = v_t \left( \frac{\partial u_i}{\partial x_j} + \frac{\partial u_j}{\partial x_i} \right) \frac{\partial u_i}{\partial x_i}$$

$$v_t = C_\mu \frac{k^2}{\epsilon}$$

The coefficients in the  $k$ - $\epsilon$  turbulence model is given as follows:

$$C_1 = \max \left[ 0.43 \frac{\mu}{(\mu_t + 5)}, C_2 = 1.0, \sigma_k = 1.0, \sigma_\epsilon = 1.2 \right]$$

To achieve the realizability effect,  $C_\mu$  is no longer constant, but a function of turbulence fields, mean strain, and rotation rates.

The SIMPLE algorithm along with Green Gauss Node Based method is used for simulations.

The SIMPLE algorithm uses a relationship between velocity and pressure corrections to enforce mass conservation and to obtain the pressure field.

When the Green-Gauss theorem is used to compute the gradient of the scalar volume fraction  $\phi$  at the cell center  $c_0$ , the discrete form is written as,

$$(\nabla \phi)_{c_0} = \frac{1}{v} \sum_f \bar{\phi}_f \bar{A}_f$$

Where  $\bar{\phi}_f$  is the value of  $\phi$  at the cell face centroid  $N_f$  is the number of nodes on the face.

In Green Gauss Node Based method, the gradient is evaluated by taking the arithmetic average of the nodal values on the face.

$$\phi_f = \frac{1}{N_f} \sum_n \bar{\phi}_n$$

The residual values were set to 0.001 for all variables except energy, which was set to  $1e-6$ . The under-relaxation factors are set to 0.3, 1, 1, 0.7, and 0.8 for pressure, density, body forces, momentum, and turbulent kinetic energy respectively.

#### 4. Boundary Conditions

Mass flow inlets are used at both hot and cold sides. The outlets are set to pressure-outlets with a fixed value of 0 Pa, so that the inlet pressure becomes equal to the pressure drop for both the streams. The outside walls of the shell were made adiabatic.

The material of shell domain as well as tube was set to steel. The hot and cold fluid domains were defined with inlet and outlet name selections. The cases where the inlet temperature of the hot fluid was  $50^\circ\text{C}$  and  $70^\circ\text{C}$ , and the cold fluid inlet being  $31^\circ\text{C}$  were investigated. The mass flow rate of the hot stream and the cold stream was varied from 0.00833 kg/s to 0.0333 kg/s.

#### 5. Model Validation

To validate the computational model used in this present investigation, the outlet temperature of the hot and cold fluid is estimated computationally. For model validation, flow and geometric conditions are selected as given in the experimental matrix.

The inlet temperature of the hot fluid was set to  $50^\circ\text{C}$  and the cold fluid inlet being  $31^\circ\text{C}$ . The mass flow rate of the hot fluid was kept constant at 0.01667 kg/s and the mass flow rate of the cold fluid was varied from 0.01667 kg/s to 0.0333 kg/s in equal intervals.

The results obtained using computational and experimental methodology are compared and shown in **Fig. 4** and **Fig. 5**.

The graphs obtained show very close resemblance. The variations between the experimental and computational results are within 5% which is well within the range.

This validates our computational model and methodology adopted in the present investigation for selected geometry and flow conditions.

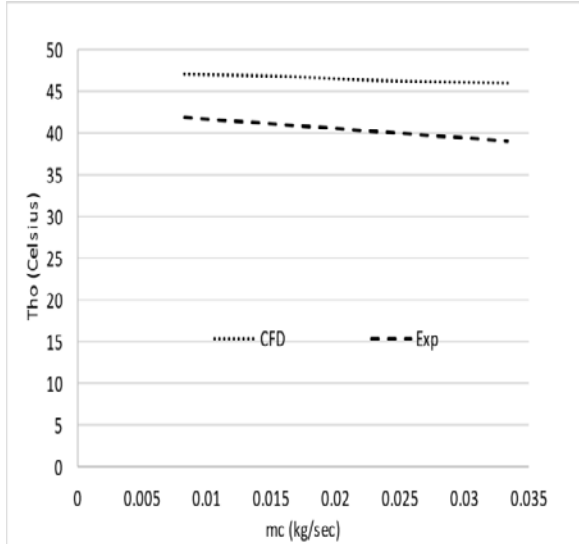


Fig. 5 Outlet temperature of the cold fluid vs mass flow rate of cold fluid



Fig. 6. Experimental setup of the double pipe heat exchanger

**B. Experimental Methodology**

The given figure (Fig. 6) demonstrates the setup on which the experiment was performed. It is a double pipe heat exchanger which when adjusted properly gives us the arrangement for either parallel flow or counter flow.

There are two heaters present, each of 500W for heating of water as hot fluid. Similarly, there are two rota meters each calibrated up to 10LPM measuring the flow rate of the hot and cold fluid.

There is also a dimmer-stat with a digital display present which when rotated to the appropriate position gives us the

temperature of the hot or cold fluid at the outlet position or the inlet position. To proceed with the experiment, first, the water is allowed to flow through the piped to the rotameter.

The desired flow rate of the hot and cold fluid is set and then the heater is switched on. Depending on the inlet conditions, the heater is run for the corresponding amount of time and when it is achieved the readings are accordingly taken.

If we want to perform the same experiment for different inlet temperatures, the heater is switched off and the inlet temperature of the hot fluid is allowed to come to room temperature and then again, the heater is switched on and readings are taken at the desired temperature.

**1. Experimental Matrix**

TABLE II THE FOLLOWING TABLE INDICATES THE EXPERIMENTAL MATRIX DEVELOPED FOR DIFFERENT INLET, FLOW, AND TEMPERATURE CONDITIONS.

Q hot	(lpm)	0.5							
Q cold		0.5	1	1.5	2	0.5	1	1.5	2
Inlet Temperature	Thi	50				70			
	Tci	34	33	32	31	34	33	32	31

Q hot	(lpm)	1							
Q cold		0.5	1	1.5	2	0.5	1	1.5	2
Inlet Temperature	Thi	50				70			
	Tci	31	32	31	31	31	31	31	31

Q hot	(lpm)	1.5							
Q cold		0.5	1	1.5	2	0.5	1	1.5	2
Inlet Temperature	Thi	50				70			
	Tci	31	31	31	31	31	31	31	31

Q hot	(lpm)	2							
Q cold		0.5	1	1.5	2	0.5	1	1.5	2
Inlet Temperature	Thi	50				70			
	Tci	31	31	31	31	31	31	31	31

### IV. RESULTS AND DISCUSSIONS

The following chapter discusses the comparative study between the numerical results and experimental data.

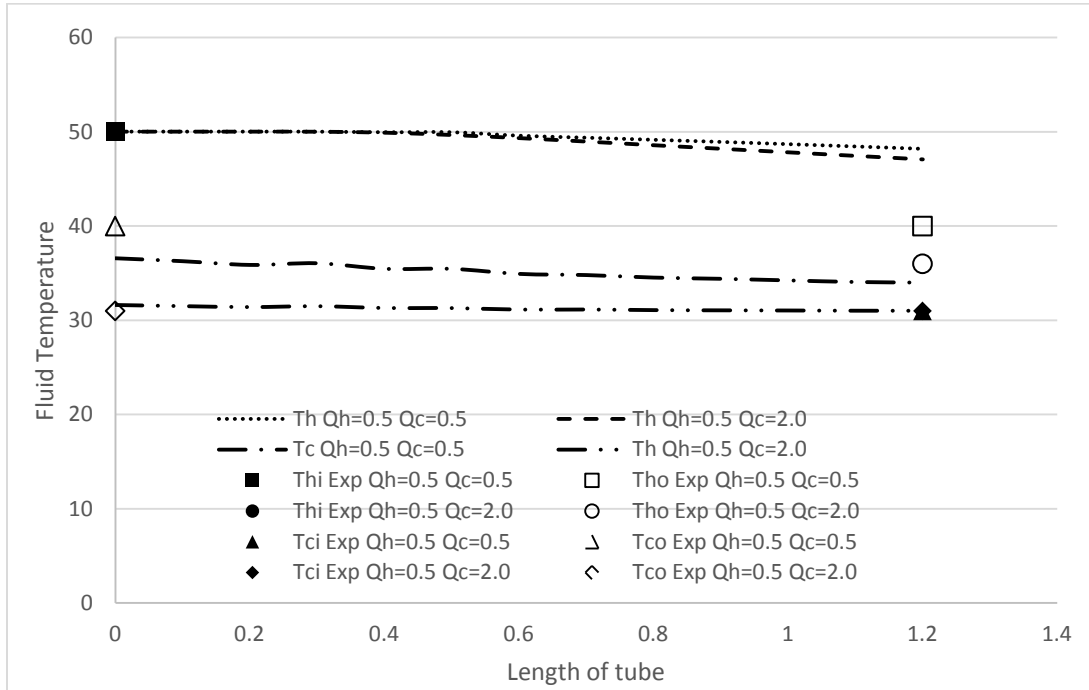


Fig. 7 Fluid Temperature v/s Length plot for the hot fluid flow rate of 0.5 lpm at 50°C for different cold flow rates.

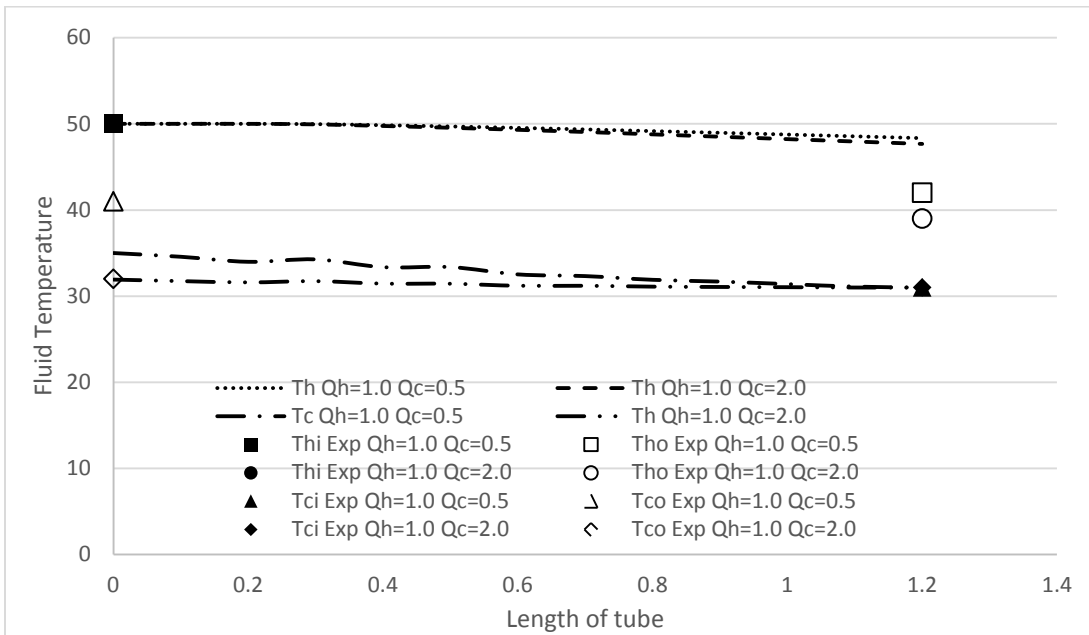


Fig.8 Fluid Temperature v/s Length plot for the hot fluid flow rate of 1.0 lpm at 50°C for different cold flow rates.

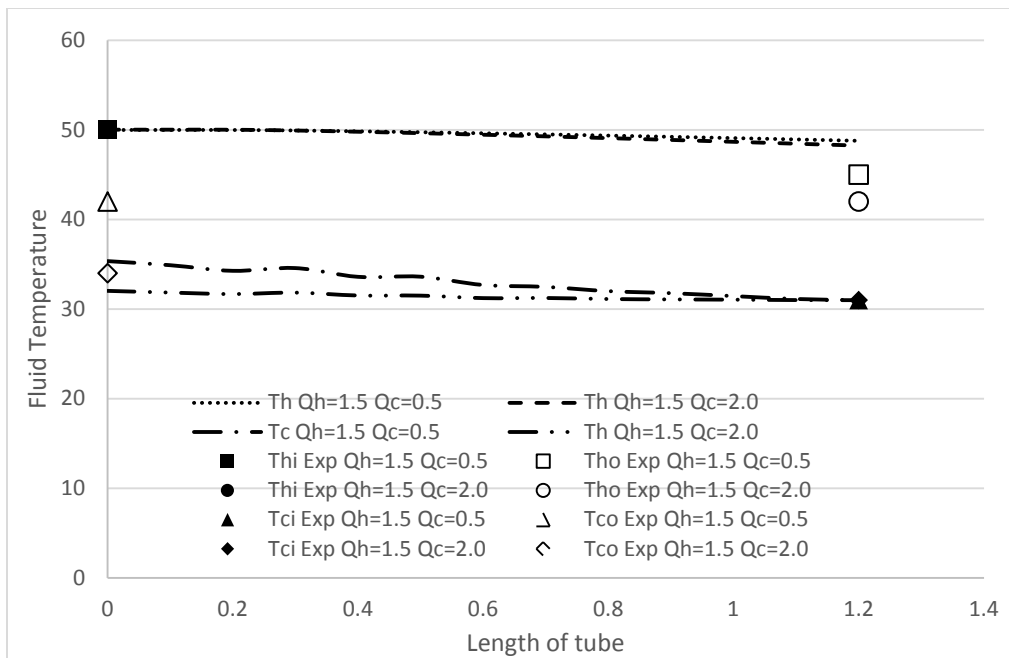


Fig. 9 Fluid Temperature v/s Length plot for the hot fluid flow rate of 1.5 lpm at 50°C for different cold flow rates.

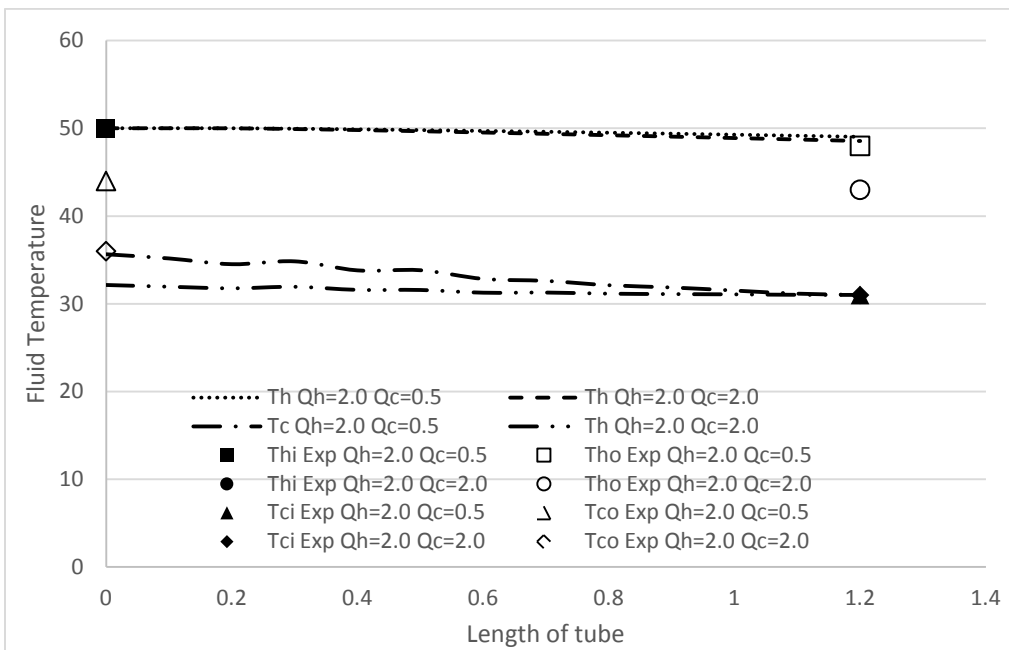


Fig. 10 Fluid Temperature v/s Length plot for the hot fluid flow rate of 2.0 lpm at 50°C for different cold flow rates.

Fig. 7, Fig. 8, Fig. 9, and Fig. 10 show the variation of temperature along the length for a particular hot fluid flow rate and different cold flow rates.

At 50°C, the temperature at the hot outlet decreases progressively with the increase in cold flow rate. As the cold fluid flow rate increases, the heat-carrying capacity of the fluid increases, and more heat transfer takes place.

The singular points depict the experimental values for the same conditions. The difference between these values can

be accounted for the environmental errors and other random factors. It can be observed that the rate of decrease of the hot fluid temperature with an increase in flow rate has decreased considerably.

This means that any further increase in the flow rate would not help further reduction in temperature. Finally, the rate of decrease becomes constant.

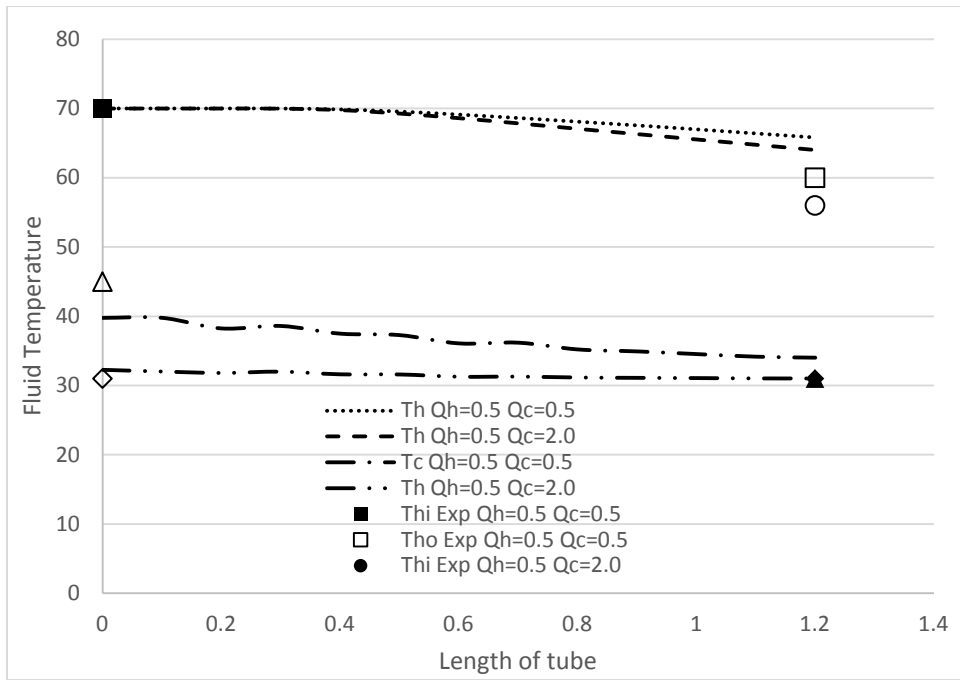


Fig. 11 Fluid Temperature v/s Length plot for the hot fluid flow rate of 0.5 lpm at 70°C for different cold flow rates.

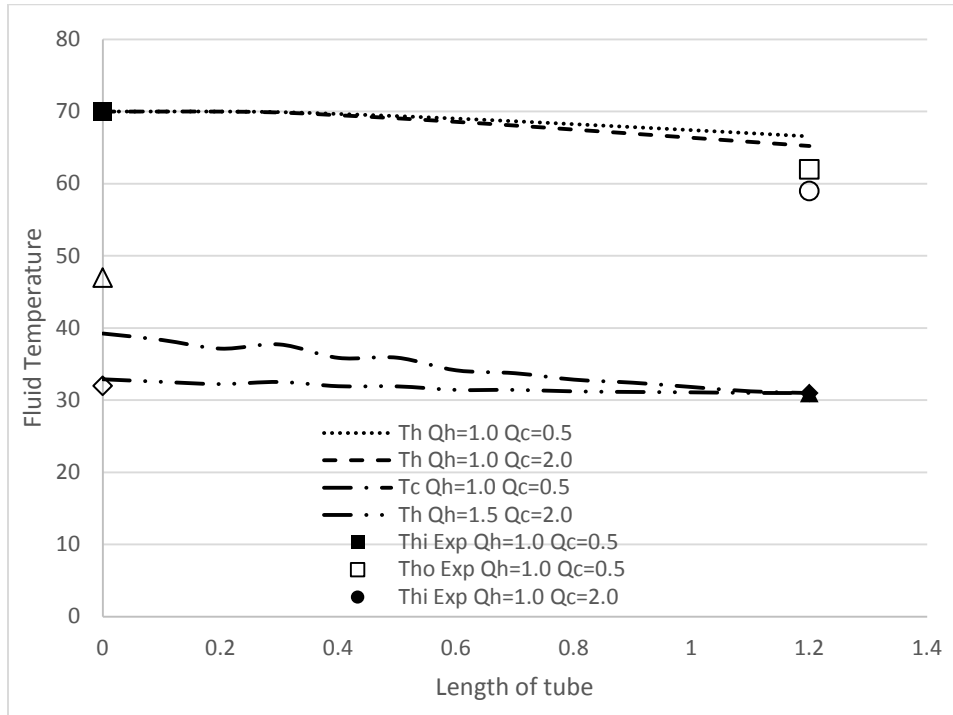


Fig. 12 Fluid Temperature v/s Length plot for the hot fluid flow rate of 1.0 lpm at 70°C for different cold flow rates.



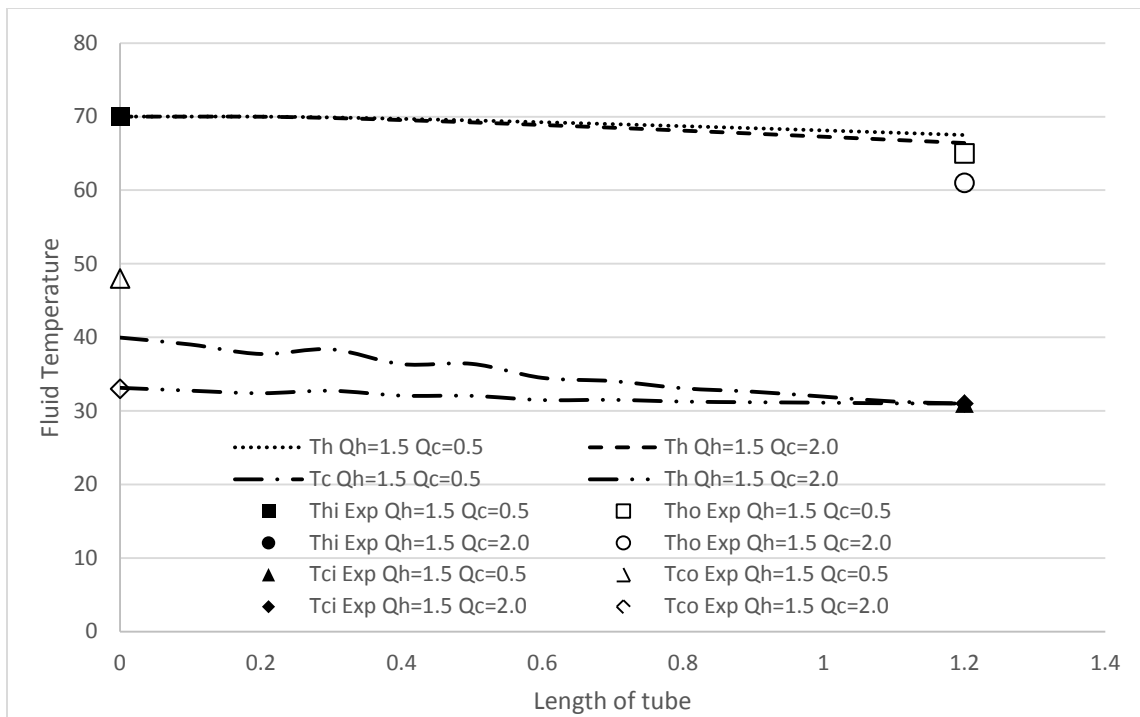


Fig.13 Fluid Temperature v/s Length plot for the hot fluid flow rate of 1.5 lpm at 70°C for different cold flow rates.

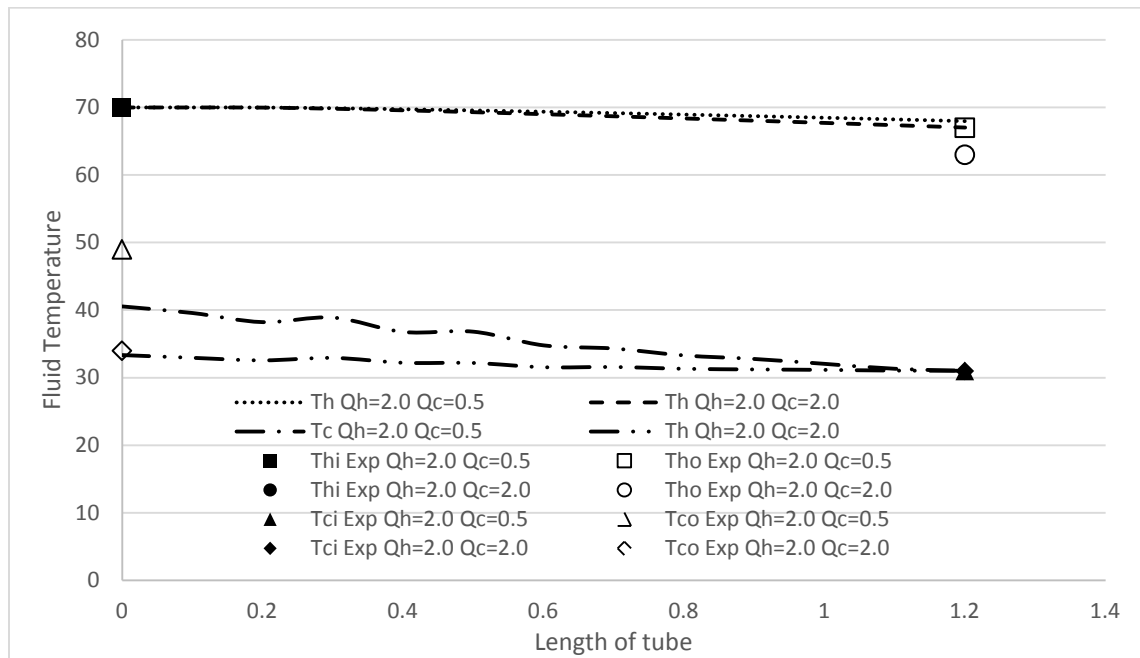


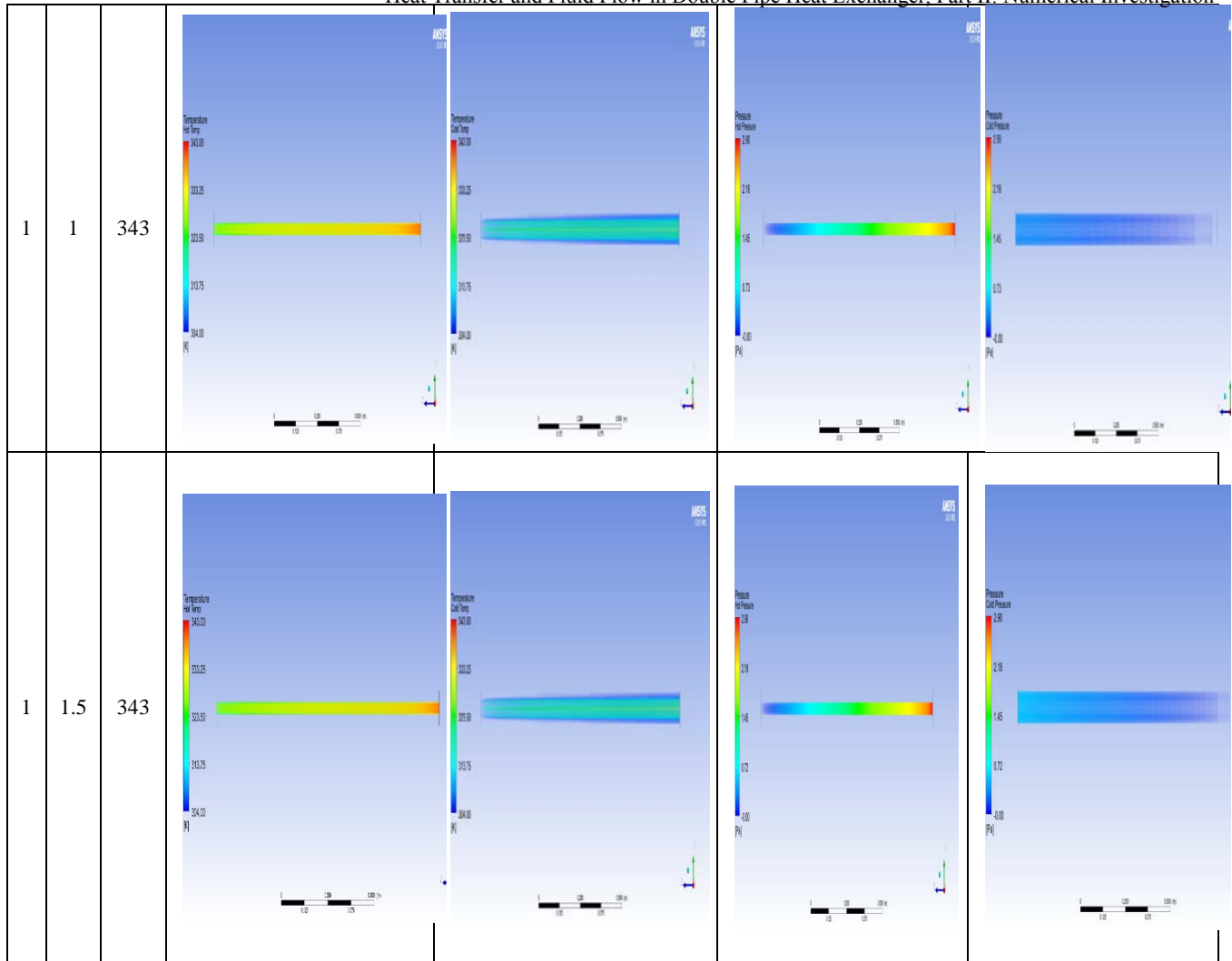
Fig.14 Fluid Temperature v/s Length plot for the hot fluid flow rate of 2.0 lpm at 70°C for different cold flow rates.

The above set of graphs *i.e.* Fig. 11, Fig. 12, Fig. 13, and Fig. 14 show the variation of temperature along the length for fixed hot fluid flow rate and different cold flow rates. At 70°C, the temperature at the hot outlet decreased

progressively with the increase in cold flow rate. These are similar conditions as for 50°C, but as the initial temperature difference is greater, it attains a constant heat transfer rate for slightly higher flow rates.

TABLE III THE FOLLOWING TABLE REPRESENTS THE TEMPERATURE AND PRESSURE CONTOURS OF THE HOT AND COLD FLUID AT DIFFERENT FLOW CONDITION

Inlet Conditions			Temperature		Pressure	
$Q_h$	$Q_c$	$T_{hi}$ (K)	Hot	Cold	Hot	Cold
1	0.5	343				
1	2	343				



## V. CONCLUSION

The effect of changing the inlet temperature of the hot fluid on the thermo-hydraulic characteristics of a double pipe heat exchanger under different working conditions is investigated in the present study. The testing conditions are run at Reynolds numbers ranging from 60 to 240. The experimental results as well as the numerical observations indicate that changing the inlet temperature of the hot fluid

has a significant effect on the thermal characteristics like outlet temperature of the hot and cold fluid. It was observed that as the difference in temperatures increases, the rate of heat transfer also increases. As we increase the flow rate of cold fluid for a fixed hot fluid flow rate, the outlet temperature of the hot fluid decreases.

This happens until a certain value of saturation is reached i.e., the temperature of hot fluid does not decrease even when the flow rate of cold fluid is increased. Hence further decrease in temperature is not possible. With a higher initial temperature difference, the heat transfer rate is higher but decreases and becomes almost constant as the flow rate is increased. Hence the hot fluid may be cooled only up to a certain temperature within specified limits. The CFD

analysis for the shell and tube heat exchanger was done and the results were obtained as above. The comparison between the CFD and experimental values show close relation between simulated and practical phenomenon with a deviation of about 10%. The values for each case have been obtained after several iterations until stable results were seen. The boundary conditions and parametric equations were set according to the requirement to maintain the same conditions as the physical experiment.

## REFERENCES

- [1] S.Kakac, H. Liu and A. Pramuanjaroenkij, Heat Exchangers Selection, Rating and Thermal Design, Third Edition, CRC Press, 2012.
- [2] F.P. Incropera and D.P. Dewitt, Introduction to Heat Transfer, Wiley, 1996.
- [3] D.Q. Kern, Process Heat Transfer, International Student Edition, McGraw-Hill International Book Company, 21st Edition, 1983.
- [4] Y.A. Cengel and A.J. Ghajar, Heat and Mass Transfer: Fundamentals and Applications, Fifth Edition, McGraw-Hill Education, 2015.
- [5] K.M. Shirvan, R. Ellahi, S. Mirzakanlari and M. Mamourian, "Enhancement of heat transfer and heat exchanger effectiveness in a double pipe heat exchanger filled with porous media: Numerical simulation and sensitivity analysis of turbulent fluid flow," *Applied Thermal Engineering*, Vol. 109A, pp. 761-774, 2016.

- [6] A.E. Maakoul, K. Feddi, S. Saadeddine, A.B. Abdellah, and M.E. Metoui, "Performance enhancement of finned annulus using surface interruptions in double-pipe heat exchangers," *Energy Conversion and Management*, Vol. 210, pp.112710, 2020.
- [7] M. Cavazzuti, A. Elia and A.M. Corticelli, "Optimization of a finned concentric pipes heat exchanger for industrial recuperative burners," *Applied Thermal Engineering*, Vol. 84, pp. 110-117, 2015.
- [8] J.T. Rennie and G.S.V. Raghavan, "Numerical studies of a double pipe helical heat exchanger," *Applied Thermal Engineering*, Vol. 26, pp. 1266-1273, 2006.
- [9] A.E. Maakoul, M.E. Metoui, A.B. Abdellah, S. Saadeddine and M. Meziane, "Numerical investigation of thermohydraulic performance of air to water double-pipe heat exchanger with helical fins," *Applied Thermal Engineering*, Vol. 127, pp. 127-139, 2017.
- [10] A.E. Maakoul, A. Laknizi, S. Saadeddine, A.B. Abdellah, M. Meziane and M.E. Metoui, "Numerical design and investigation of heat transfer enhancement and performance for an annulus with continuous helical baffles in a double-pipe heat exchanger," *Applied Thermal Engineering*, Vol. 133, pp. 76-86, 2017.
- [11] M. Sheikholeslami, D.D. Ganji and M.G. Bandpy, "Experimental and numerical analysis for effects of using conical ring on turbulent flow and heat transfer in a double pipe air to water heat exchanger," *Applied Thermal Engineering*, Vol. 100, pp. 805-819, 2016.
- [12] W. Tu, Y. Wang and Y. Tang, "A numerical study on thermal-hydraulic characteristics of turbulent flow through a circular tube fitted with pipe inserts," *Applied Thermal Engineering*, Vol. 101, pp. 413-421, 2016.
- [13] M. Bezaatpour and M. Goharkhah, "Convective heat transfer enhancement in a double pipe mini heat exchanger by magnetic field induced swirling flow," *Applied Thermal Engineering*, Vol. 167, 114801, 2020.
- [14] I. Bashtani and J.A. Esfahani, "ε-NTU analysis of turbulent flow in a corrugated double pipe heat exchanger: A numerical investigation," *Applied Thermal Engineering*, Vol. 159, pp.113886, 2019.
- [15] S. Zhang, L. Lu, C. Dong and S.H. Cha, "Thermal characteristics of perforated self-rotating twisted tapes in a double-pipe heat exchanger," *Applied Thermal Engineering*, Vol. 162, pp.114296, 2019.
- [16] K. Sharifi, M. Sabeti, M. Rafiei, A.H. Mohammadi and L. Shirazi, "Computational Fluid Dynamics (CFD) Technique to Study the Effects of Helical Wire Inserts on Heat Transfer and Pressure Drop in a Double Pipe Heat Exchanger," *Applied Thermal Engineering*, Vol. 128, pp. 898-910, 2018.
- [17] A.T. Wijayanta, I. Yaningsih, M. Aziz, T. Miyazaki and S. Koyama, "Double-sided delta-wing tape inserts to enhance convective heat transfer and fluid flow characteristics of a double-pipe heat exchanger," *Applied Thermal Engineering*, Vol. 145, pp. 27-37, 2018.
- [18] A. Bazgir, N. Nabhani and S. Eiamsa-ard, "Numerical analysis of flow and thermal patterns in a double-pipe Ranque-Hilsch vortex tube: Influence of cooling a hot-tube," *Applied Thermal Engineering*, Vol. 144, pp. 181-208, 2018.
- [19] J.M. Gorman, K.R. Krautbauer and E.M. Sparrow, "Thermal and fluid flow first-principles numerical design of an enhanced double pipe heat exchanger," *Applied Thermal Engineering*, Vol. 107, pp. 194-206, 2016.